inorganics

MDPI

Article

Rare Nuclearities in Ni(II) Cluster Chemistry: An Unprecedented {Ni_{12}} Nanosized Cage from the Use of *N*-Naphthalidene-2-Amino-5-Chlorobenzoic Acid

Panagiota S. Perlepe [1], Konstantinos N. Pantelis [2], Luís Cunha-Silva [3], Vlasoula Bekiari [4], Albert Escuer [5] and Theocharis C. Stamatatos [1,2,*]

1 Department of Chemistry, Brock University, 1812 Sir Isaac Brock Way, St. Catharines, ON L2S 3A1, Canada; pennyperlepes@gmail.com
2 Chemistry Department, University of Patras, 265 04 Patras, Greece; kostaspantelis95@gmail.com
3 LAQV/REQUIMTE & Department of Chemistry and Biochemistry, Faculty of Sciences, University of Porto, 4169-007 Porto, Portugal; l.cunha.silva@fc.up.pt
4 School of Agricultural Sciences, University of Patras, 30200 Messolonghi, Greece; bbekiari@upatras.gr
5 Departament de Quimica Inorgànica i Orgànica, Secció Inorgànica and Institut de Nanociència i Nanotecnologia (IN2UB), Universitat de Barcelona, Martí Franqués 1-11, 08028 Barcelona, Spain; albert.escuer@qi.ub.es
* Correspondence: thstama@upatras.gr; Tel.: +30-2610-996008

Received: 10 March 2020; Accepted: 6 May 2020; Published: 9 May 2020

Abstract: The self-assembly reaction between NiI_2, benzoic acid ($PhCO_2H$) and the Schiff base chelate, *N*-naphthalidene-2-amino-5-chlorobenzoic acid ($nacbH_2$), in the presence of the organic base triethylamine (NEt_3), has resulted in the isolation and the structural, spectroscopic, and physicochemical characterization of the dodecanuclear $[Ni_{12}I_2(OH)_6(O_2CPh)_5(nacb)_5(H_2O)_4(MeCN)_4]I$ (**1**) cluster compound in ~30% yield. Complex **1** has a cage-like conformation, comprising twelve distorted, octahedral Ni^{II} ions that are bridged by five μ_3-OH^-, one μ-OH^-, an I^- in 55% occupancy, five $PhCO_2^-$ groups (under the η^1:η^1:μ, η^1:η^2:μ_3 and η^2:η^2:μ_4 modes), and the naphthoxido and carboxylato O-atoms of five doubly deprotonated $nacb^{2-}$ groups. The overall {Ni_{12}} cluster exhibits a nanosized structure with a diameter of ~2.5 nm and its metallic core can be conveniently described as a series of nine edge- or vertex-sharing {Ni_3} triangular subunits. Complex **1** is the highest nuclearity coordination compound bearing the $nacbH_2$ chelate, and a rare example of polynuclear Ni^{II} complex containing coordinating I^- ions. Direct current (DC) magnetic susceptibility studies revealed the presence of predominant antiferromagnetic exchange interactions between the Ni^{II} ions, while photophysical studies of **1** in the solid-state showed a cyan-to-green centered emission at 520 nm, upon maximum excitation at 380 nm. The reported results demonstrate the rich coordination chemistry of the deprotonated $nacb^{2-}$ chelate in the presence of Ni^{II} metal ions, and the ability of this ligand to adopt a variety of different bridging modes, thus fostering the formation of high-nuclearity molecules with rare, nanosized dimensions and interesting physical (i.e., magnetic and optical) properties.

Keywords: polynuclear metal complexes; nickel(II); schiff base ligands; *N*-naphthalidene-2-amino-5-chlorobenzoic acid; single-crystal X-ray crystallography; molecular magnetism; emission studies

1. Introduction

Polynuclear 3d-metal complexes (or 3d-metal clusters) remain one of the most attractive research fields in the cross-disciplinary areas of chemistry, physics, and materials science [1]. This is mainly due to the ability of these nanosized molecular species to exhibit very interesting magnetic, optical, biological, and catalytic properties, to name just a few [2]. From a structural perspective, the motifs

of these cluster compounds often resemble the aesthetically beautiful structures of highly-symmetric inorganic solids, such as cubic and hexagonal structures, perovskites, brucites, and supertetrahedra, due to the presence of multiple bridging oxido and hydroxido groups [3]. In the molecular magnetism arena, ferromagnetically-coupled 3d-systems with a large ground state spin value, *S*, and an appreciable magnetic anisotropy of the Ising (or easy-axis) type can behave as single-molecule magnets (SMMs) [4]. SMMs exhibit slow magnetization relaxation over and/or through an anisotropy barrier and they represent a molecular or "bottom-up" approach to nanoscale magnetism with potential applications in the fields of information storage, molecular electronics and spintronics [5].

The first and most well-studied family of SMMs is the mixed-valence $[Mn^{III}_8Mn^{IV}_4O_{12}(O_2CR)_{16}(X)_4]$, where RCO_2^- and X are various carboxylate bridging groups and terminal solvate molecules, respectively [6]. The SMM behavior of these compounds originates from the combined $S = 10$ spin ground state and the enhanced magnetic anisotropy resulting from the parallel alignment of the Mn^{III} Jahn-Teller axes. In polynuclear Ni^{II} cluster chemistry, the number of SMMs is substantially smaller [7] and only a few of them show slow relaxation of magnetization in the absence of an external DC field, as well as magnetization hysteresis, the diagnostic property of a magnet. This is predominately due to the small zero-field splitting parameter, *D*, that a polynuclear Ni^{II} complex often exhibits when the Ni^{II} atoms adopt the favorable octahedral coordination geometry. Exceptional examples of Ni^{II} cluster-based SMMs are the ferromagnetic $[Ni_{12}(chp)_{12}(O_2CMe)_{12}(THF)_6(H_2O)_6]$ with a ring-like topology [8], and the family of $[Ni_4(hmp)_4(ROH)_4Cl_4]$ complexes with a distorted cubane $[Ni_4(OR)_4]^{4+}$ core [9], where chpH and hmpH are the organic chelates chloro-2-hydroxypyridine and 2-hydroxymethylpyridine, respectively, and ROH are various terminally-bound alcohol solvates.

It becomes apparent that the choice of the organic chelating/bridging ligand is of fundamental importance in the self-assembly synthesis of high-nuclearity Ni^{II} complexes with high-spin values and interesting magnetic dynamics. To this end, we have recently started a research program aiming at the exploration of Schiff base chelates, which are based on the tridentate *N*-salicylidene-*o*-aminophenol ($saphH_2$, Scheme 1) scaffold, in 3d-metal cluster chemistry as a means of obtaining nanosized molecular materials, primarily those with interesting magnetic properties [10]. To increase the coordination and bridging potential of the organic chelate, we initially turned our attention to the tetradentate ligand *N*-salicylidene-2-amino-5-chlorobenzoic acid ($sacbH_2$, Scheme 1); this has led to the structurally impressive $\{Ni_{18}\}$ and $\{Ni_{26}\}$ clusters [11], and a $\{Dy_2\}$ SMM with a large energy barrier for magnetization reversal [12]. A reasonable leap forward would be the replacement of the phenyl ring of the *N*-salicylidene moiety with a naphthalene one. The resulting ligand *N*-naphthalidene-2-amino-5-chlorobenzoic acid ($nacbH_2$, Scheme 1) shows the following salient features: (a) it is still a tetradentate like $sacbH_2$, but is undoubtedly more rigid and sterically demanding than $sacbH_2$, and (b) it includes the naphthalene substituent, a well-known fluorescent group [13], which could open new prospects in the emission properties of Ni^{II} coordination compounds with *O*- and *N*-donor atoms. Both features presage the synthesis of new cluster compounds with potentially interesting magnetic and emission properties. Indeed, the initial employment of $nacbH_2$ in Ni^{II} chemistry has afforded a series of $\{Ni_5\}$ and $\{Ni_6\}$ clusters with diverse magnetic and optical properties, but with limited bridging affinity for $nacb^{2-}$ [14]. In this work, we have unveiled the bridging capacity of $nacb^{2-}$ in conjunction with ancillary bridging benzoate groups. We herein report an unprecedented $\{Ni_{12}\}$ cluster compound with the highest nuclearity in metal cluster chemistry of $nacbH_2$, and one of the rarest nuclearities in Ni^{II} cluster chemistry.

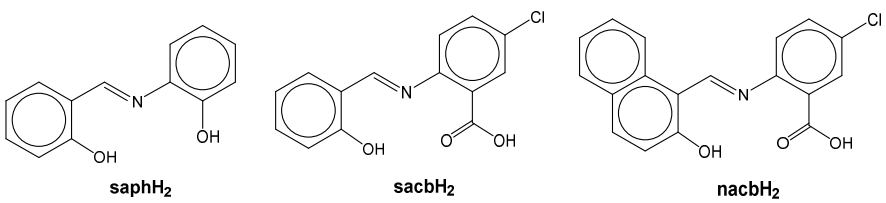

Scheme 1. Structural formulae and abbreviations of the Schiff base ligands discussed in the text.

2. Results and Discussion

2.1. Synthetic Comments

The general reaction system NiX_2/nacbH_2, where X^- are various anions with either a strong (i.e., NO_3^-, β-diketonates and pseudohalides) or weak coordinating (Cl^-, Br^- and ClO_4^-) ability, has been studied by us [15], and—in almost all the cases—small in nuclearity clusters (i.e., {Ni_5} and {Ni_6}) were isolated and structurally characterized [14]. These results have demonstrated the unpredictability of the nacbH_2 chelate toward the coordination with 3d-metal ions in solution and subsequently the stabilization of different cluster compounds in the solid-state. We have thus decided to introduce to the Ni^{II}/nacbH_2 system anions with very limited coordinating capacity, such as iodides (I^-), in conjunction with organic anionic groups with a superior bridging ability, such as benzoates ($PhCO_2^-$), in an attempt to harness a flexible "synthetic blend" which would potentially lead to high-nuclearity Ni^{II} clusters. Indeed, the reaction between NiI_2, nacbH_2, $PhCO_2H$, and NEt_3 in a 2:1:1:3 molar ratio, in solvent acetonitrile (MeCN), afforded dark-green crystals of the dodecanuclear cluster compound $[Ni_{12}I_2(OH)_6(O_2CPh)_5(nacb)_5(H_2O)_4(MeCN)_4]I$ (**1**) in 30% yield. The general formation of **1** is summarized by the following stoichiometric Equation (1).

$$\begin{gathered} 12\ NiI_2 + 5\ nacbH_2 + 5\ PhCO_2H + 21\ NEt_3 + 10\ H_2O + 4\ MeCN \rightarrow \\ [Ni_{12}I_2(OH)_6(O_2CPh)_5(nacb)_5(H_2O)_4(MeCN)_4]I + 21\ NHEt_3I \end{gathered} \quad (1)$$

Under the context of chemical reactivity, several synthetic parameters were explored to either increase the yield of the isolated product **1** or alter the nuclearity of the {Ni_{12}} compound and subsequently isolate a new product. In particular, the employment of $NiCl_2$ or $NiBr_2$ in place of NiI_2 afforded the already reported $(NHEt_3)_2[Ni_6(OH)_2(nacb)_6(H_2O)_4]$ [14], whereas the replacement of $PhCO_2H$ by other carboxylic acids, such as $MeCO_2H$ or $EtCO_2H$, led to green-colored microcrystalline products, of which we were unable to determine the crystal structures due to the very small size of the obtained crystallites. The presence of NEt_3 as an external base was also essential for the clean preparation of **1**, providing a proton acceptor to facilitate the complete deprotonation of nacbH_2 and $PhCO_2H$, and fostering the metal-assisted deprotonation of H_2O molecules in solution to the coordinating OH^- groups (*vide infra*). Various similar reactions in other organic solvents (i.e., alcohols (ROH), CH_2Cl_2 and mixtures of MeCN/ROH) and/or external bases (i.e., trimethylamine (NMe_3), tripropylamine (NPr_3), diethylamine (Et_2NH), dimethylamine (Me_2NH) and tetramethylammonium hydroxide (Me_4NOH) yielded amorphous solids that we were unable to recrystallize and further characterize. Finally, it is worth mentioning that the presence of iodide ions, either as bound groups or counterions, or both, in Ni^{II} coordination chemistry is limited to a handful of previously reported dinuclear or trinuclear compounds [16–19].

2.2. Description of Structure

A partially labeled representation of the cation of complex **1** is shown in Figure 1. The positively charged cluster cation $[Ni_{12}I_2(OH)_6(O_2CPh)_5(nacb)_5(H_2O)_4(MeCN)_4]^+$ is counterbalanced by an I^- anion in the crystal lattice of **1**. The I^- counterion (I7) is closely held with the {Ni_{12}} cluster through H-bonding interactions with three of the bridging OH^- groups; these separations are: O1···I7 = 3.226(3) Å, O2···I7 = 3.425(1) Å and O3···I7 = 3.222(3) Å. Selected interatomic distances and angles of **1** are listed in Table 1. Bond valence sum (BVS) calculations for the inorganic bridging O-atoms with 100% occupancies gave values of: 1.23 (for O1), 1.16 (for O2 and O8), 1.10 (for O4), and 1.18 (for O9), in excellent agreement with their assignment as OH^- groups. Oxygen BVS values in the ~1.7–2.0, ~1.0–1.2, and ~0.2–0.4 ranges are indicative of non-, single- and double-protonation, respectively [20].

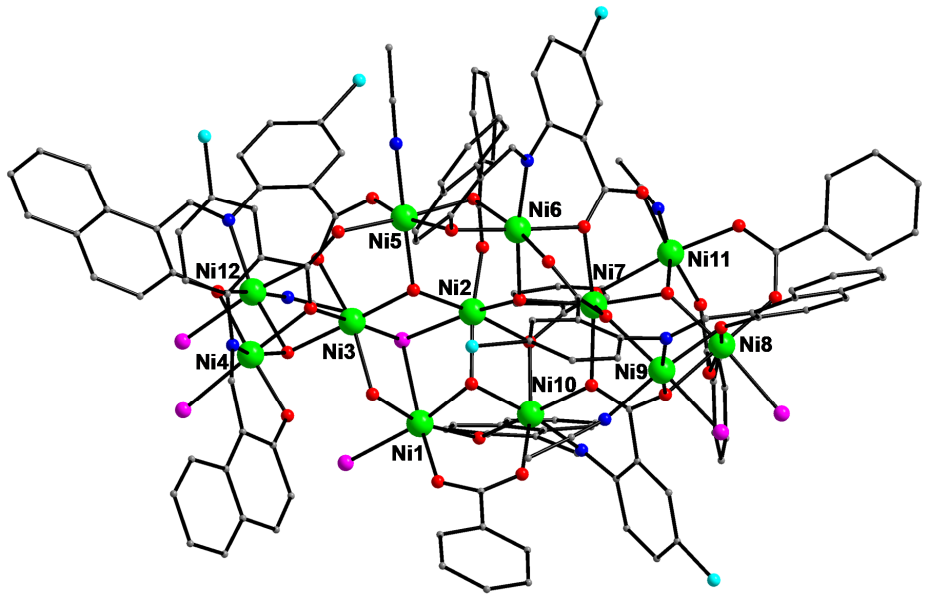

Figure 1. Partially labeled representation of the cation of complex **1**. Color scheme: Ni^{II}: green; Cl: cyan; I: purple; O: red; N: blue; C: gray. H atoms are omitted for clarity.

Table 1. Selected interatomic distances (Å) and angles (°) for complex **1**.

Bond	Distances	Bond	Distances	Bond	Angles	Bond	Angles
Ni1–O1	1.994(5)	Ni7–O8	2.017(5)	Ni3–I1–Ni2	78.6(4)	Ni2–O8–Ni6	116.0(2)
Ni1–O26	2.020(6)	Ni7–O9	2.017(5)	Ni3–I1–Ni1	81.6(4)	Ni7–O8–Ni6	99.2(2)
Ni1–O15	2.087(5)	Ni7–O23	2.114(5)	Ni2–I1–Ni1	78.4(4)	Ni8–O9–Ni7	126.9(3)
Ni1–O3	2.151(6)	Ni7–O17	2.128(5)	Ni1–O1–Ni10	96.6(2)	Ni8–O9–Ni11	112.0(3)
Ni1–I2	2.484(2)	Ni7–O12	2.137(5)	Ni1–O1–Ni2	112.8(2)	Ni7–O9–Ni11	102.8(2)
Ni1–I1	2.643(1)	Ni7–O14	2.176(5)	Ni10–O1–Ni2	104.7(2)	Ni9–O10–Ni8	98.8(2)
Ni2–O1	2.005(5)	Ni8–O21	2.005(6)	Ni3–O2–Ni5	113.3(2)	Ni9–O11–Ni8	99.2(2)
Ni2–O8	2.007(5)	Ni8–O9	2.006(5)	Ni3–O2–Ni2	107.2(2)	Ni9–O12–Ni7	113.7(2)
Ni2–O27	2.014(5)	Ni8–O19	2.031(6)	Ni5–O2–Ni2	120.9(2)	Ni10–O14–Ni7	118.6(2)
Ni2–O2	2.057(5)	Ni8–O11	2.113(6)	Ni3–O3–Ni1	103.8(2)	Ni10–O15–Ni1	92.9(2)
Ni2–O16	2.134(5)	Ni8–O10	2.138(6)	Ni3–O4–Ni12	101.5(2)	Ni2–O16–Ni10	95.3(2)
Ni2–I1	2.628(1)	Ni8–I4	2.479(5)	Ni3–O4–Ni4	97.5(2)	Ni7–O17–Ni11	91.2(2)
Ni3–O2	2.001(5)	Ni9–N1	1.988(7)	Ni12–O4–Ni4	99.4(2)	Ni6–O23–Ni7	97.4(2)
Ni3–O4	2.040(6)	Ni9–O10	2.025(6)	Ni3–O5–Ni4	94.9(2)	Ni6–O24–Ni5	100.7(2)
Ni3–O5	2.061(5)	Ni9–O11	2.039(6)	Ni6–O7–Ni5	94.9(2)	Ni3–O29–Ni12	99.6(2)
Ni3–O29	2.063(5)	Ni9–N2	2.092(8)	Ni2–O8–Ni7	119.0(2)	Ni12–O30–Ni4	99.2(2)
Ni3–O3	2.150(5)	Ni9–O12	2.117(5)				
Ni3–I1	2.532(1)	Ni9–I5	2.367(9)				
Ni4–O31	1.996(6)	Ni10–N3	1.994(6)				
Ni4–N9	2.016(7)	Ni10–O1	2.000(5)				
Ni4–O4	2.049(5)	Ni10–O15	2.026(5)				
Ni4–O30	2.069(6)	Ni10–O25	2.039(6)				
Ni4–O5	2.113(5)	Ni10–O14	2.126(5)				
Ni4–I3	2.498(5)	Ni10–O16	2.158(5)				
Ni5–O2	2.011(5)	Ni11–O20	2.015(6)				
Ni5–O24	2.063(5)	Ni11–O18	2.016(6)				
Ni5–O28	2.064(6)	Ni11–O9	2.019(6)				
Ni5–O6	2.066(5)	Ni11–O22	2.050(6)				
Ni5–N8	2.093(7)	Ni11–N5	2.115(9)				
Ni5–O7	2.126(5)	Ni11–O17	2.283(5)				
Ni6–O24	1.997(5)	Ni12–N6	2.024(7)				
Ni6–O23	2.002(5)	Ni12–O30	2.030(6)				
Ni6–N4	2.013(6)	Ni12–O4	2.045(6)				
Ni6–O8	2.044(5)	Ni12–N7	2.076(8)				
Ni6–O13	2.052(5)	Ni12–O29	2.081(5)				
Ni6–O7	2.120(5)	Ni12–I6	2.482(4)				

Complex **1** is a closed cage-like cluster consisting of 12 Ni^{II} ions that are bridged by five μ_3-OH^-, one μ-OH^-, an I^- in 55% occupancy, and the naphthoxido and carboxylato O-atoms of five double-deprotonated $nacb^{2-}$ groups. The latter are arranged into three classes (Figure 2), with all of them acting as tridentate chelates to a Ni^{II} ion, and additionally bridging two (η^1:η^1:η^2:η^1:μ_3 mode), three (η^2:η^1:η^2:η^1:μ_4 mode) and four (η^2:η^1:η^2:η^2:μ_5 mode) metal ions. The variety of binding modes of $nacb^{2-}$ in complex **1** clearly emphasizes the coordination affinity of this Schiff base ligand with Ni^{II} ions, and its ability to stabilize high-nuclearity 3d-metal clusters with unprecedented structural motifs and nanosized dimensions. To this end, the space-filling plot (Figure 3) shows that **1** has a nearly "bowl"-shaped conformation with the longest intramolecular C···C distance being ~25 Å, excluding the H atoms. The shortest Ni···Ni distance between neighboring $\{Ni_{12}\}$ clusters in the crystal is 12.246(2) Å, thus confirming the good separation of the cluster compounds due to the bulky naphthalene substituents of the $nacb^{2-}$ ligands.

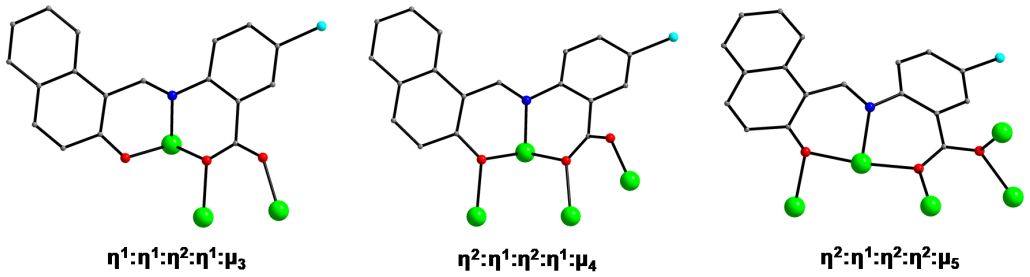

Figure 2. Crystallographically established coordination modes of $nacb^{2-}$ ligands present in complex **1**. Color scheme as in Figure 1.

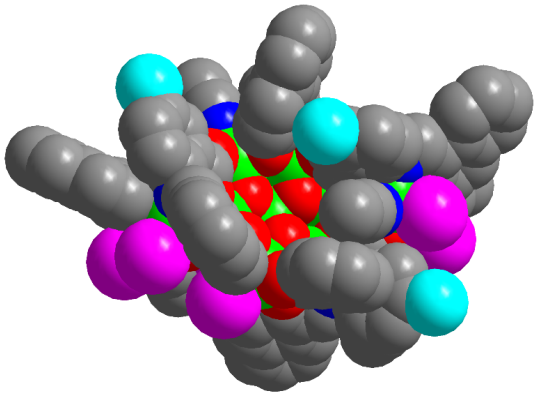

Figure 3. Space-filling representation of **1**. Color scheme as in Figure 1.

Additional bridging about the twelve Ni^{II} ions is provided by five $PhCO_2^-$ groups, which are arranged into three classes; three of them are bridging under the η^1:η^1:μ mode, one is acting as an η^1:η^2:μ_3 ligand, and the last one adopts the rare η^2:η^2:μ_4 mode. Thus, the resulting core is $[Ni_{12}(\mu_3\text{-}OH)_5(\mu_3\text{-}I/H_2O)(\mu\text{-}OR)_{15}]^{3+}$ (Figure 4), and peripheral ligation about this core is further provided by four terminally bound MeCN molecules (on Ni5, Ni9, Ni11, and Ni12) and a total of five I^-/H_2O group combinations (on Ni1, Ni4, Ni8, Ni9, and Ni12). All Ni^{II} atoms are six-coordinate with distorted octahedral geometries. The metallic core of **1** can be conveniently described as a series of nine edge- or vertex-sharing $\{Ni_3\}$ triangular subunits (Figure 5), which are held together by μ_3-OH^- and μ-OR^- groups. An alternative description of the $\{Ni_{12}\}$ metal arrangement is that of a central $\{Ni_7\}$ subunit possessing a distorted disk-like topology [Ni(1,2,3,5,6,7,10)], which is attached to a $\{Ni_3\}$ triangular [Ni(3,4,12)] and a $\{Ni_4\}$ rhombus-shaped [Ni(7,8,9,11)] subunits by sharing the common Ni3 and Ni7 vertices, respectively. Finally, the nuclearity of complex **1** is the largest reported to date of a metal cluster bearing $nacb^{2-}$ chelate, and it joins a relatively rare family of $\{Ni_{12}\}$ Werner-type compounds with a cage-like conformation [21–24].

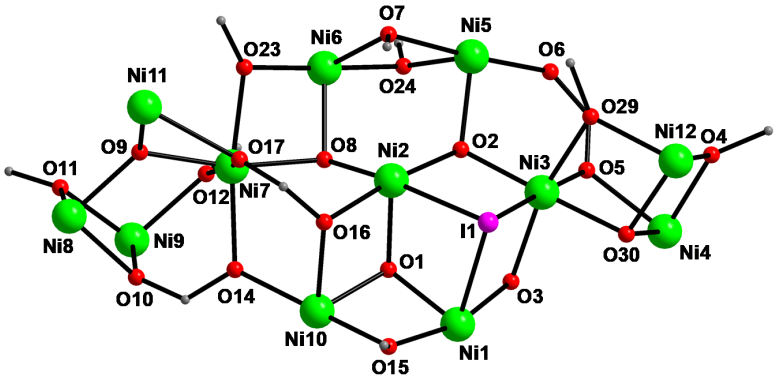

Figure 4. Complete, labelled core of the {Ni_{12}} cluster. Color scheme as in Figure 1.

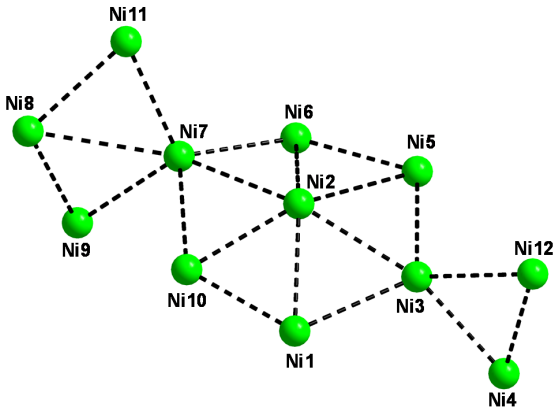

Figure 5. Metal topology of the {Ni_{12}} cluster; the black dashed lines are virtual bonds to emphasize the edge- and vertex-sharing {Ni_3} triangles.

2.3. Solid-State Magnetic Susceptibility Studies

Variable-temperature (2.0–300 K range), direct-current (DC) magnetic susceptibility measurements were performed on a freshly-prepared microcrystalline solid of **1** under a weak DC field of 0.03 T to avoid saturation effects. The data are shown as $\chi_M T$ versus T plot in Figure 6. The value of the $\chi_M T$ product at 300 K is 10.40 cm^3 $Kmol^{-1}$, slightly lower than the value of 12 cm^3 $Kmol^{-1}$ (calculated with g = 2.0) expected for twelve non-interacting, high-spin Ni^{II} (S = 1) atoms. Upon cooling, the $\chi_M T$ product continuously decreases down to a value of 3.06 cm^3 $Kmol^{-1}$ at 2 K. A slightly different curvature of the plot is observed below ~5 K, and this likely due to the onset of zero-field splitting, intermolecular antiferromagnetic interactions between the {Ni_{12}} clusters, and/or Zeeman effects [11,15]. The overall shape of the $\chi_M T$ versus T plot is suggestive of the presence of predominant antiferromagnetic exchange interactions between the metal centers, as frequently observed in many high-nuclearity and low-symmetry Ni^{II} cage-like clusters where many different magnetic exchange pathways are in effect [11]. To this end, a fit of the experimental data to a theoretical model ($H = -2J_{ij}\hat{S}_i \cdot \hat{S}_j$ convention) was not feasible. Undoubtedly, **1** possesses a small ground-state spin value, with the $\chi_M T$ value at 2 K being consistent with an S ~ 2 ground state (for g = 2). The antiferromagnetic response of the {Ni_{12}} compound can be tentatively assigned to the majority of obtuse Ni–O–Ni bond angles (close to or larger than 100°) and the presence of {Ni_3} triangular subunits, which are prone to spin frustration effects [25]. Magnetization (M) versus field (H) measurements (Figure 6, inset) at 2 K show a continuous increase of M as the field increases, reaching a non-saturated value of 6.0 $N\mu_B$ at 5 T; this is likely due to the presence of low-lying excited states, as reported previously for other high-nuclearity Ni^{II} complexes [26]. As a result, attempts to fit the reduced magnetization data assuming that only the ground state is populated were very poor.

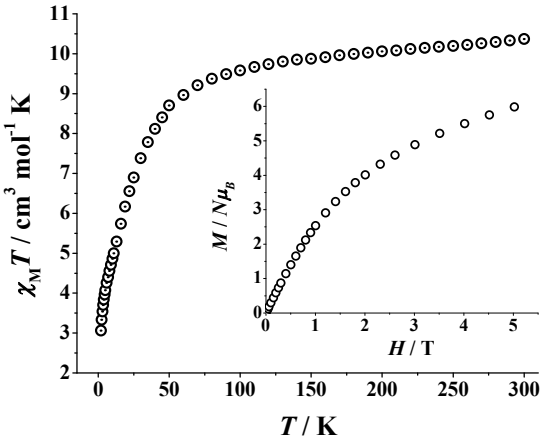

Figure 6. Temperature dependence of the $\chi_M T$ product for complex **1** at 0.03 T. (inset) Plot of magnetization (M) versus field (H) for **1** at 2 K.

2.4. Solid-State Emission Studies

The photophysical properties of complex **1** were carried out in the solid-state and at room temperature due to its structural instability in solution. This was confirmed by performing electrospray ionization mass spectrometry (ESI-MS) studies in various solvent media (Figure S1). The optical response of the free-ligand nacbH_2 has been reported by us in a previous work [15]. Briefly, it was shown that nacbH_2 is a promising "antenna" group for the promotion of energy transfer effects. Upon maximum excitation at ~350 nm, nacbH_2 exhibits a strong emission in the visible range with two clear maxima at ~390 and 410 nm, and a weak shoulder at ~480 nm. Complex **1** shows an interesting photophysical response, given its large nuclearity, the presence of many different binding groups, and the possible quenching effects from the coordinating O- and N-atoms. The dodecanuclear compound **1** exhibits a cyan-to-green centered emission at 520 nm, upon maximum excitation at 380 nm (Figure 7). The red-shifted emission of **1** with respect to the free nacbH_2 can be tentatively assigned to the coordination of the deprotonated nacb^{2-} ligands with the metal ions and/or the presence of additional binding groups with emission efficiency, such as benzoates, which could affect the charge transfer process and resulting emission [14,15].

In general, the loss of energy due to vibrations is reduced as a result of the coordination of a ligand to a metal center; this binding enhances the organic ligand's rigidity [27]. In addition, the usually observed optical quenching effects from the paramagnetic metal ions can be prevented using organic fluorescent groups, such as the naphthalene, anthracene, and phenanthrene substituents [28]. Red-shifted emissions are commonly observed in most fluorescent compounds in the solid-state, likely due to the π–π stacking interactions of the aromatic rings [29]. Due to the structural complexity of **1**, as a result of the many different ligands present and the number of metal ions, among other electronic and steric perturbations, an in-depth analysis of the photophysical properties of **1** would be unrealistic.

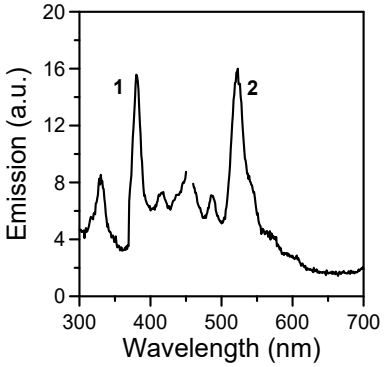

Figure 7. Excitation (1) and emission (2) spectra of complex **1** in the solid-state and at room temperature.

3. Materials and Methods

3.1. Materials, Physical and Spectroscopic Measurements

All manipulations were performed under aerobic conditions using materials (reagent grade) and solvents as received unless otherwise noted. The Schiff base ligand nacbH_2 was prepared, purified, and characterized as described elsewhere [14,15]. Elemental analyses (C, H, and N) were performed on a Perkin-Elmer 2400 Series II Analyzer (Foster City, CA, USA). Infrared spectra were recorded in the solid state on a Bruker's FT-IR spectrometer (ALPHA's Platinum ATR single reflection) (Billerica, MA, USA) in the 4000–400 cm^{-1} range. Excitation and emission spectra were recorded in the solid state at room temperature conditions using a Cary Eclipse spectrofluorometer. The repeatability and reproducibility of the emission was verified by recording the emission spectra of the material three times in two different days using the same scan rate and the same excitation and emission monochromator slits. Variable-temperature magnetic susceptibility studies were performed on a MPMS5 Quantum Design magnetometer equipped with a 5 T magnet and operating in the 2–300 K range. The microcrystalline sample was embedded in solid eicosane to prevent torquing. Diamagnetic corrections were applied to the observed paramagnetic susceptibility using Pascal's constants [30].

*3.2. Synthesis of [$Ni_{12}I_2(OH)_6(O_2CPh)_5(nacb)_5(H_2O)_4(MeCN)_4$]I (**1**)*

To a stirred, orange suspension of nacbH_2 (0.07 g, 0.20 mmol) in MeCN (20 mL) was added NEt_3 (84 µL, 0.60 mmol). Solids NiI_2 (0.13 g, 0.40 mmol) and $PhCO_2H$ (0.03 g, 0.20 mmol) were added to the resulting yellow solution, and a noticeable color change to a dark-green solution was observed over the period of 1 h, under a continuous magnetic stirring. The final solution was filtered, and the filtrate was carefully layered with Et_2O (40 mL). After 20 days, X-ray quality dark-green plate-like crystals of **1** were formed, and these were collected by filtration, washed with cold MeCN (2 × 3 mL) and Et_2O (2 × 3 mL), and dried in air. The yield was 30% (based on the ligand available). The air-dried solid was found to be slightly hygroscopic and it was satisfactorily analyzed as **1**·3H_2O. Anal. calc. for $C_{133}H_{107}N_9O_{38}Ni_{12}Cl_5I_3$ (found values in parentheses): C 43.16% (43.31%), H 2.91% (3.06%), N 3.41% (3.28%). Selected IR data (ATR): ν = 3300 (mb), 1598 (s), 1575 (s), 1535 (s), 1503 (w), 1472 (m), 1450 (m), 1427 (m), 1406 (s), 1382 (w), 1337 (s), 1298 (m), 1249 (m), 1217 (m), 1180 (m), 1156 (m), 1113 (m), 1088 (m), 985 (m), 961 (w), 885 (w), 852 (m), 828 (m), 743 (s), 718 (s), 670 (w), 630 (w), 555 (w), 451 (m).

3.3. Single-Crystal X-ray Crystallography

A suitable single-crystal of complex **1** was selected and mounted on the respective cryoloop using adequate inert oil [31]. Diffraction data were collected on a Bruker X8 Kappa APEX II Charge-Coupled Device (CCD) area-detector diffractometer (Billerica, MA, USA) controlled by the APEX2 software [32] package (Mo Kα graphite-monochromated radiation, λ = 0.71073 Å), and equipped with an Oxford Cryosystems Series 700 cryostream, monitored remotely with the software interface Cryopad [33]. Images were processed with the software SAINT+ [34], and the absorption effects were corrected by the multi-scan method implemented in SADABS [35]. The structure was solved using the algorithm implemented in SHELXT-2014 [36,37], and refined by successive full-matrix least-squares cycles on F^2 using the latest SHELXL-v.2014 [36,38]. The non-hydrogen atoms of the crystal structure were successfully refined using anisotropic displacement parameters, and H-atoms bonded to carbon of the ligands were placed at their idealized positions using appropriate *HFIX* instructions in SHELXL. All these atoms were included in subsequent refinement cycles in riding-motion approximation with isotropic thermal displacement parameters (U_{iso}) fixed at 1.2 or 1.5 × U_{eq} of the relative atom. The refinement model revealed the presence of two coordinated iodide (I^-) ions and four coordinated H_2O molecules partially disordered over six coordinative positions with distinct complementary occupancies (I1/O1W = 0.55/0.45; I2/O2W = 0.35/0.65; I3/O3W = 0.30/0.70; I4/O4W = 0.25/0.75; I5/O5W = 0.25/0.75, and I6/O6W = 0.30/0.70). In addition, the non-coordinated I^- ion is disordered over two positions with occupancies of 0.65 and 0.35. As a result of the severely disordered structure

of **1**, the H-atoms of the coordinated water molecules and hydroxido groups were not included in the refined model, but they were considered in the final molecular formula of the compound.

Substantial electron density was found on the data of complex **1**, most probably due to additional disordered solvate molecules occupying the spaces originated by the close packing of the cluster compound. Various efforts to properly locate, model, and refine these residues were unsuccessful, and the examination for the total potential solvent area using the software package PLATON [39] clearly confirmed the existence of cavities with potential solvent accessible void volume. Thus, the original data set was treated with the program SQUEEZE [40], which calculates the contribution of the smeared electron density in the lattice voids and adds this to the calculated structure factors from the structural model when refining against the hkl file. The programs used for molecular graphics were MERCURY [41] and DIAMOND [42]. Unit cell parameters, structure solution and refinement details for **1** are summarized in Table 2. Further crystallographic details can be found in the corresponding CIF file provided in the ESI. Crystallographic data (excluding structure factors) for the structure reported in this work have been deposited to the Cambridge Crystallographic Data Centre (CCDC) as supplementary publication number: CCDC-1988904. Copies of the data can be obtained online using https://summary.ccdc.cam.ac.uk/structure-summary-form.

Table 2. Crystallographic data for complex **1**.

Parameter	1
Empirical formula	$C_{133}H_{101}N_9O_{35}Ni_{12}Cl_5I_3$
FW/g mol^{-1}	3647.69
Temperature/K	150(2)
Crystal type	Green plate
Crystal size/mm^3	0.22 × 0.10 × 0.04
Crystal system	Triclinic
Space group	*P*-1
a/Å	19.422(2)
b/Å	22.654(3)
c/Å	25.321(3)
α/°	115.783(4)
β/°	92.992(5)
γ/°	109.118(5)
Volume/Å^3	9443(2)
Z	2
ρ_{calc}/g cm^{-3}	1.283
μ/mm^{-1}	1.786
F(000)	3644
θ range/°	3.65 to 25.03
Radiation	Mo Kα (λ = 0.71073)
Index ranges	$-23 \le h \le 22$ $-22 \le k \le 26$ $-30 \le l \le 30$
Reflections collected	134,933
Independent reflections	32,481 (R_{int} = 0.0476)
Goodness-of-fit on F^2	1.040
Final R indexes [$I \ge 2\sigma(I)$] [a,b]	R_1 = 0.0872 wR_2 = 0.2099
Final R indexes [all data]	R_1 = 0.1221 wR_2 = 0.2361
$(\Delta\rho)_{max,min}$/e Å^{-3}	1.613 and −1.594

[a] $R_1 = \sum(||F_o| - |F_c||)/\sum|F_o|$. [b] $wR_2 = [\sum[w(F_o^2 - F_c^2)^2]/\sum[w(F_o^2)^2]]^{1/2}$, $w = 1/[\sigma^2(F_o^2) + (ap)^2 + bp]$, where $p = [\max(F_o^2, 0) + 2F_c^2]/3$.

4. Conclusions and Perspectives

In conclusion, we have herein reported the synthesis, and structural and physicochemical characterization, of a new dodecanuclear Ni^{II} cluster compound with an unprecedented structural motif and nanoscale dimensions, resulted from the successful employment of the nacbH_2/I^-/PhCO_2^- "ligand blend" in Ni^{II} chemistry. The *N*-naphthalidene-2-amino-5-chlorobenzoic acid (nacbH_2) ligand also contributed to the observation of unquenched optical emission from the {Ni_{12}} complex **1** in the solid-state, a very unusual phenomenon in high-nuclearity 3d-metal cluster chemistry with

N-/O-donor atoms. Complex **1** is by far the highest nuclearity Ni^{II} cluster compound with coordinating I^- ions, also supported by ancillary chelating and bridging organic groups, thus presaging a new synthetic approach to nanoscale molecular materials with interesting structural motifs and physical properties. We are currently investigating the $Ni^{II}/RCO_2^-/nacbH_2$ tertiary system as a means of obtaining higher-nuclearity, nanosized Ni^{II} clusters with interesting magneto-optical properties.

Supplementary Materials: The CIF and the checkCIF output files of complex **1** are available online at http://www.mdpi.com/2304-6740/8/5/32/s1. Figure S1. Positive ion ES mass spectrum of **1** in a solvent mixture of $MeCN/CH_2Cl_2$.

Author Contributions: P.S.P. and K.N.P. conducted the syntheses, crystallization, purification, optimization, conventional characterization and interpretation of the structural and magnetic data of complex **1**; L.C.-S. collected single-crystal X-ray diffraction data, solved the structure and performed the complete refinement; V.B. collected, plotted, rationalized and discussed the optical properties of complex **1**; A.E. collected, plotted and discussed magnetic and part of the spectroscopic data of the compound; T.C.S. coordinated the research, contributed to the interpretation of the results and wrote the paper based on the reports of his collaborators; All the authors exchanged ideas and comments regarding the explanation of the results and discussed upon the manuscript at all stages. All authors have read and agreed to the published version of the manuscript.

Funding: This research was funded by NSERC-DG and ERA to T.C.S. P.S.P thanks the Alexander S. Onassis Public Benefit Foundation for a graduate scholarship. L.C.-S. thanks the Fundação para a Ciência e a Tecnologia (FCT/Ministério da Ciência, Tecnologia e Ensino Superior, Portugal) for the financial support to the LAQV/REQUIMTE (UID/QUI/50006/2019) through national funds. A.E. acknowledges financial support from Ministerio de Economia y Competitividad, Project CTQ2018-094031-B-100.

Conflicts of Interest: The authors declare no conflict of interest.

References

1. Papatriantafyllopoulou, C.; Moushi, E.E.; Christou, G.; Tasiopoulos, A.J. Filling the gap between the quantum and classical worlds of nanoscale magnetism: Giant molecular aggregates based on paramagnetic 3d metal ions. *Chem. Soc. Rev.* **2016**, *45*, 1597–1628. [CrossRef] [PubMed]
2. Maayan, G.; Gluz, N.; Christou, G. A bioinspired soluble manganese cluster as a water oxidation electrocatalyst with low overpotential. *Nat. Catal.* **2018**, *1*, 48–54. [CrossRef]
3. Deng, Y.-K.; Su, H.-F.; Xu, J.-H.; Wang, W.-G.; Kurmoo, M.; Lin, S.-C.; Tan, Y.-Z.; Jia, J.; Sun, D.; Zheng, L.-S. Hierarchical assembly of a $\{Mn^{II}_{15}Mn^{III}_4\}$ brucite disc: Step-by-step formation and ferrimagnetism. *J. Am. Chem. Soc.* **2016**, *138*, 1328–1334. [CrossRef] [PubMed]
4. Holynska, M. (Ed.) *Single-Molecule Magnets: Molecular Architectures and Building Blocks for Spintronics*; Wiley-VCH: Weinheim, Germany, 2018.
5. Bogani, L.; Wernsdorfer, W. Molecular spintronics using single-molecule magnets. *Nat. Mater.* **2008**, *7*, 179–186. [CrossRef] [PubMed]
6. Bagai, R.; Christou, G. The drosophila of single-molecule magnetism: $[Mn_{12}O_{12}(O_2CR)_{16}(H_2O)_4]$. *Chem. Soc. Rev.* **2009**, *38*, 1011–1026. [CrossRef] [PubMed]
7. Milios, C.J.; Winpenny, R.E.P. Cluster-based single-molecule magnets. *Struct. Bond.* **2015**, *164*, 1–110.
8. Blake, A.J.; Grant, C.M.; Parsons, S.; Rawson, J.M.; Winpenny, R.E.P. The synthesis, structure and magnetic properties of a cyclic dodecanuclear nickel complex. *J. Chem. Soc. Chem. Commun.* **1994**, 2363–2364. [CrossRef]
9. Yang, E.-C.; Wernsdorfer, W.; Hill, S.; Edwards, R.S.; Nakano, M.; Maccagnano, S.; Zakharov, L.N.; Rheingold, A.L.; Christou, G.; Hendrickson, D.N. Exchange bias in Ni_4 single-molecule magnets. *Polyhedron* **2003**, *22*, 1727–1733. [CrossRef]
10. Alexandropoulos, D.I.; Nguyen, T.N.; Cunha-Silva, L.; Zafiropoulos, T.F.; Escuer, A.; Christou, G.; Stamatatos, T.C. Slow magnetization relaxation in unprecedented $Mn^{III}_4Dy^{III}_3$ and $Mn^{III}_4Dy^{III}_5$ clusters from the use of *N*-salicylidene-*o*-aminophenol. *Inorg. Chem.* **2013**, *52*, 1179–1181. [CrossRef]
11. Athanasopoulou, A.A.; Pilkington, M.; Raptopoulou, C.P.; Escuer, A.; Stamatatos, T.C. Structural aesthetics in molecular nanoscience: A unique Ni_{26} cluster with a 'rabbit-face' topology and a discrete Ni_{18} 'molecular chain'. *Chem. Commun.* **2014**, *50*, 14942–14945. [CrossRef] [PubMed]
12. Mazarakioti, E.C.; Regier, J.; Cunha-Silva, L.; Wernsdorfer, W.; Pilkington, M.; Tang, J.; Stamatatos, T.C. Large energy barrier and magnetization hysteresis at 5 K for a symmetric $\{Dy_2\}$ complex with spherical tricapped trigonal prismatic Dy^{III} ions. *Inorg. Chem.* **2017**, *56*, 3568–3578. [CrossRef] [PubMed]

13. Alexandropoulos, D.I.; Mowson, A.M.; Pilkington, M.; Bekiari, V.; Christou, G.; Stamatatos, T.C. Emissive molecular nanomagnets: Introducing optical properties in triangular oximato $\{Mn^{III}_3\}$ SMMs from the deliberate replacement of simple carboxylate ligands with their fluorescent analogues. *Dalton Trans.* **2014**, *43*, 1965–1969. [CrossRef] [PubMed]
14. Perlepe, P.S.; Cunha-Silva, L.; Bekiari, V.; Gagnon, K.J.; Teat, S.J.; Escuer, A.; Stamatatos, T.C. Structural diversity in Ni^{II} cluster chemistry: Ni_5, Ni_6, and $\{NiNa_2\}_n$ complexes bearing the Schiff-base ligand *N*-naphthalidene-2-amino-5-chlorobenzoic acid. *Dalton Trans.* **2016**, *45*, 10256–10270. [CrossRef] [PubMed]
15. Perlepe, P.S.; Cunha-Silva, L.; Gagnon, K.J.; Teat, S.J.; Lampropoulos, C.; Escuer, A.; Stamatatos, T.C. "Ligands-with-benefits": Naphthalene-substituted Schiff bases yielding new Ni^{II} metal clusters with ferromagnetic and emissive properties and undergoing exciting transformations. *Inorg. Chem.* **2016**, *55*, 1270–1277. [CrossRef]
16. Prema, D.; Oshin, K.; Desper, J.; Levy, C.J. Mono- and dinuclear nickel(II) complexes of resolved Schiff-base ligands with extended quinoline substituents. *Dalton Trans.* **2012**, *41*, 4998–5009. [CrossRef] [PubMed]
17. Szacilowski, K.T.; Puhui, X.; Malkhasian, A.Y.S.; Heeg, M.J.; Udugala-Ganehenege, M.Y.; Wenger, L.E.; Endicott, J.F. Solid-state structures and magnetic properties of halide-bridged, face-to-face bis-nickel(II)-macrocyclic ligand complexes: Ligand-mediated interchanges of electronic configuration. *Inorg. Chem.* **2005**, *44*, 6019–6033. [CrossRef] [PubMed]
18. Fossey, J.S.; Matsubara, R.; Kiyohara, H.; Kobayashi, S. Heterochiral triangulo nickel complex as evidence of a large positive nonlinear effect in catalysis. *Inorg. Chem.* **2008**, *47*, 781–783. [CrossRef] [PubMed]
19. Morgenstern, D.A.; Ferrence, G.M.; Washington, J.; Henderson, J.I.; Rosenhein, L.; Heise, J.D.; Fanwick, P.E.; Kubiak, C.P. A class of halide-supported trinuclear nickel clusters $[Ni_3(\mu_3\text{-L})(\mu_3\text{-X})(\mu_2\text{-dppm})_3]^{n+}$ (L = I^-, Br^-, CO, CNR.; X = I^-, Br^-; *n* = 0, 1; dppm = $Ph_2PCH_2PPh_2$): Novel physical properties and the fermi resonance of symmetric μ_3-η^1 bound isocyanide ligands. *J. Am. Chem. Soc.* **1996**, *118*, 2198–2207. [CrossRef]
20. Liu, W.; Thorp, H.H. Bond valence sum analysis of metal-ligand bond lengths in metalloenzymes and model complexes. Refined distances and other enzymes. *Inorg. Chem.* **1993**, *32*, 4102–4105. [CrossRef]
21. Efthymiou, C.G.; Cunha-Silva, L.; Perlepes, S.P.; Brechin, E.K.; Inglis, R.; Evangelisti, M.; Papatriantafyllopoulou, C. In search of molecules displaying ferromagnetic exchange: Multiple-decker Ni_{12} and Ni_{16} complexes from the use of pyridine-2-amidoxime. *Dalton Trans.* **2016**, *45*, 17409–17419. [CrossRef] [PubMed]
22. Breeze, B.A.; Shanmugam, M.; Tuna, F.; Winpenny, R.E.P. A series of nickel phosphonate-carboxylate cages. *Chem. Commun.* **2007**, 5185–5187. [CrossRef] [PubMed]
23. Feltham, H.L.C.; Clérac, R.; Brooker, S. Hexa-, hepta- and dodeca-nuclear nickel(II) complexes of three Schiff-base ligands derived from 1,4-diformyl-2,3-dihydroxybenzene. *Dalton Trans.* **2009**, 2965–2973. [CrossRef] [PubMed]
24. Pons-Balagué, A.; Piligkos, S.; Teat, S.J.; Sánchez Costa, J.; Shiddiq, M.; Hill, S.; Castro, G.R.; Ferrer-Escorihuela, P.; Sañudo, E.C. New nanostructured materials: Synthesis of dodecanuclear Ni^{II} complexes and surface deposition studies. *Chem. Eur. J.* **2013**, *19*, 9064–9071. [CrossRef] [PubMed]
25. Athanasopoulou, A.A.; Raptopoulou, C.P.; Escuer, A.; Stamatatos, T.C. Rare nuclearities in Ni(II) cluster chemistry: A Ni_{11} cage from the first use of *N*-salicylidene-2-amino-5-chlorobenzoic acid in metal cluster chemistry. *RSC Adv.* **2014**, *4*, 12680–12684. [CrossRef]
26. Papatriantafyllopoulou, C.; Diamantopoulou, E.; Terzis, A.; Tangoulis, V.; Lalioti, N.; Perlepes, S.P. High-nuclearity nickel(II) clusters: Ni_{13} complexes from the use of 1-hydroxybenzotriazole. *Polyhedron* **2009**, *28*, 1903–1911. [CrossRef]
27. Bünzli, J.-C.G.; Piguet, C. Taking advantage of luminescent lanthanide ions. *Chem. Soc. Rev.* **2005**, *34*, 1048–1077. [CrossRef]
28. Alaimo, A.; Takahashi, D.; Cunha-Silva, L.; Christou, G.; Stamatatos, T.C. Emissive $\{Mn^{III}_4Ca\}$ clusters with square pyramidal topologies: Syntheses and structural, spectroscopic, and physicochemical characterization. *Inorg. Chem.* **2015**, *54*, 2137–2151. [CrossRef]
29. Binnemans, K. Lanthanide-based luminescent hybrid materials. *Chem. Rev.* **2009**, *109*, 4283–4374. [CrossRef]
30. Bain, G.A.; Berry, J.F. Diamagnetic corrections and Pascal's constants. *J. Chem. Educ.* **2008**, *85*, 532–536. [CrossRef]
31. Kottke, T.; Stalke, D. Crystal handling at low temperatures. *J. App. Cryst.* **1993**, *26*, 615–619. [CrossRef]
32. APEX2. *Data Collection Software Version 2012.4*; Bruker AXS: Delft, The Netherlands, 2012.

33. Cryopad. *Remote Monitoring and Control, Version 1.451*; Oxford Cryosystems: Oxford, UK, 2006.
34. SAINT+. *Data Integration Engine v. 7.23a* ©; Bruker AXS: Madison, WI, USA, 1997–2005.
35. Sheldrick, G.M. *SADABS v.2.01. Bruker/Siemens Area Detector Absorption Correction Program*; Bruker AXS: Madison, WI, USA, 1998.
36. Sheldrick, G.M. A short history of SHELX. *Acta Cryst. A* **2008**, *64*, 112–122. [CrossRef] [PubMed]
37. Sheldrick, G.M. *SHELXT, Version 2014/3*; Program for Crystal Structure Solution; University of Göttingen: Gottingen, Germany, 2014.
38. Sheldrick, G.M. *SHELXL, Version 2014*; Program for Crystal Structure Refinement; University of Göttingen: Gottingen, Germany, 2014.
39. Spek, A.L. *PLATON*, An integrated tool for the analysis of the results of a single crystal structure determination. *Acta Cryst. A* **1990**, *46*, C34.
40. Spek, A.L. Crystal structure refinement with *SHELXL*. *Acta Cryst.* **2015**, *C71*, 3–8.
41. Bruno, I.J.; Cole, J.C.; Edgington, P.R.; Kessler, M.K.; Macrae, C.F.; McCabe, P.; Pearson, J.; Taylor, R. New software for searching the Cambridge structural database and visualizing crystal structures. *Acta Cryst.* **2002**, *B58*, 389–397. [CrossRef] [PubMed]
42. Bradenburg, K. *DIAMOND, Release 3.1f*; Crystal Impact GbR: Bonn, Germany, 2008.